

IMAGES OF PERIODIC TRIANGULAR WAVE OBJECTS THROUGH SEA WATER

BY K. SINGH*, K. N. CHOPRA AND A. K. DIMRI

Department of Physics, Indian Institute of Technology, New Delhi**

(Received May 5, 1970; Revised paper received August 29, 1970)

The imagery of a general periodic and incoherent triangular wave grating has been investigated when sea water is considered to be the image degrading medium. Results in the form of curves have been presented for the irradiance distribution and contrast in the images.

1. Introduction

Recently, a lot of interest has been shown [1-7] in the studies of the optical properties of sea water. The modulation transfer function (MTF) approach has also been applied [8-11] to study these properties. The MTF of sea water is helpful when predicting the underwater visibility and has been computed by Zaneveld and Beardsley [9]. Goodell [10] has given a method for calculating the reflection and emission characteristics of the ocean surface as an MTF whose characteristics are functions of downlook. Wells [11] has studied the loss of resolution in water as a result of multiple small angle scattering.

These investigations [8-11], however, make use of objects with sinusoidal and rectangular wave profiles and no investigations seem to have been carried out with the use of triangular wave objects. The use of triangular wave objects has recently become quite popular for MTF studies. Singh and Chopra [12-14] have considered the triangular wave gratings for their investigations, in which they have also discussed the superiority of such objects over other types of objects. In view of the increasing use of this type of objects, we have investigated the degradation of the images of general periodic triangular wave objects through sea water, and this paper presents the results of our investigations. Knowledge of these results should prove useful in physical oceanography.

* Address: (All correspondence may please be addressed to K. Singh), Temporarily at the Applied Optics Section, Imperial College of Science and Technology, London, S.W.7, United Kingdom.

** Address: Department of Physics Indian Institute of Technology, New Delhi, 29, India.

2 Theory

For our investigations, we have considered a general periodic object of triangular wave form. The Fourier series representation of this object function $G(z)$ Fig. 1 and the image irradiance distribution $H(z')$ are given [12] by

$$G(z) = a - b + 2\alpha b + \frac{4b}{\pi^2\alpha} \sum_{n=1}^{\infty} \frac{\sin^2 n\pi\alpha}{n^2} \cos n\omega z \quad (1)$$

and

$$H(z') = a - b + 2\alpha b + \frac{4b}{\pi^2\alpha} \sum_{n=1}^{n'} f(n\omega) \frac{\sin^2 n\pi\alpha}{n^2} \cos n\omega z' \quad (2)$$

where $n = 1, 2, 3 - \alpha p$ and $(1 - \alpha)p$ are the widths of the bright and dark portions at the mean irradiance a , and b denotes the modulation. ω is the angular frequency and is given

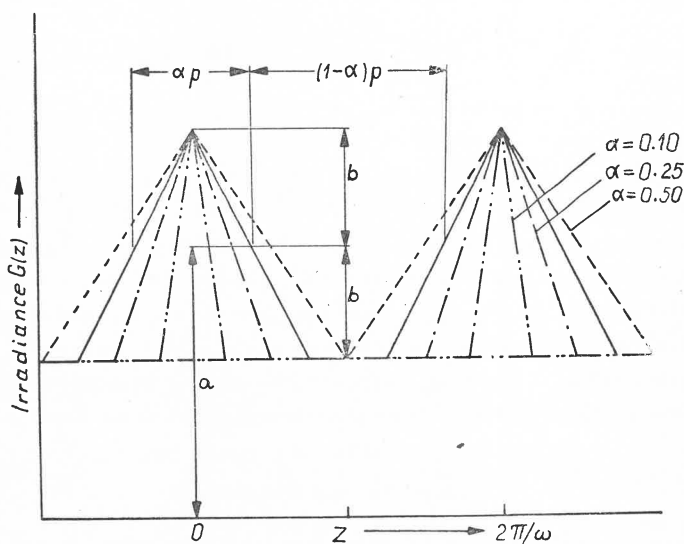


Fig. 1. Illustration of symbols

by $\omega = 2\pi/p$ where p is the period. $f(n\omega)$ is a function which for $n = 1$ reduces to the MTF of the system. The number n' of the components transmitted through the system decreases as the value of ω increases. In writing Eq. (2) the conditions of isoplanatism and unit magnification have been assumed.

In our study, we consider a simple viewing situation. The hydrosol occupies, a volume extending from $X = 0$ to $X = +\infty$; $-\infty < z < \infty$; $-\infty < y < \infty$. The observing system is located on the X axis at $X = +X_0$. The target is effectively located at $X = -\infty$. The results obtained for other viewing situations are, however, expected to be quite similar in functional form to those obtained for this simple viewing situation.

Considering the hydrosol as a set of thin horizontal plane parallel slabs of equal thickness, the edge gradient response of the system is the intersection of the image radiance solid with the $\Phi = 0^\circ, 180^\circ$ plane when the object radiance $N_0(\theta, \Phi)$ is given [9] by

$$\begin{aligned} N_0(\theta, \Phi) &= N_0; 0^\circ < \theta \leq 90^\circ, -90^\circ < \Phi < +90^\circ \\ &= 0; 0^\circ < \theta \leq 90^\circ, +90^\circ < \Phi < +270^\circ \end{aligned} \quad (3)$$

The edge gradient response can be approximately represented in the region $-20^\circ < \theta < 20^\circ$ by an arc — tangent function. The MTF is the Fourier transform of the derivative of this arc — tangent function and is given [9] by

$$f(\omega) = \exp\left(-\frac{\omega}{\omega_0}\right) \quad (4)$$

where ω is the angular frequency in cycles/degree and ω_0 is a complicated function of the range, scattering albedo and shape of the scattering phase function, and is given by

$$\omega_0 = \left(\frac{1}{\theta}\right) \tan\left[\pi\left(\frac{N_j(\theta) - N_j(0)}{2N_j(0)}\right)\right]. \quad (5)$$

Here, θ denotes the angle, N is the radiance and j is the number of layers from the surface. The pertinent optical properties of sea water are the beam extinction coefficient c' , the total scattering coefficient b' and the shape of the scattering indicatrix $\beta(\gamma)$. The constant ω_0 of the MTF is a function of the scattering indicatrix parameter's ef and eb' and the scattering albedo b'/c' . The values of $f(n\omega)$ to be used in Eq. (2) can be obtained by replacing ω by $n\omega$ in Eq. (4). It should be noted here that in writing Eq. (4), the light collector has been assumed to be perfect. If the effect of the light collecting system is also considered, then Eq. (4) should be multiplied by the appropriate MTF.

Assuming the contrast in the object equal to unity, the image contrast can be computed by calculating the maximum and minimum values of $H(z')$ from Eq. (2).

3. Results and discussion

The irradiance distribution in the images has been computed for $\alpha = 0.10, 0.25$ and 0.50 . In these calculations, the values of ω have been taken equal to $0.20, 0.90$ and 1.80 and the constant $\omega_0 = 0.05, 0.30$ and 0.50 . The parameters a and b have been taken so that $a = b = 0.50$.

Fig. 2 shows the dependence of irradiance on the reduced distance $\omega z'$. The dot-dash lines ($\cdots\cdots$) represent the edges of the geometrical images. Fig. 3 shows the effect of the change in the value of ω_0 on the normalized irradiance for $\omega = 0.60$ and 1.20 . It is seen that a decrease in ω_0 results in the deterioration of the image contrast at all frequencies.

The sequence of curves in Fig. 4 shows the contrast in the images of the triangular wave grating for $\omega_0 = 0.20$ and 0.50 . The curves marked S give the contrast in the images of the sine wave grating and have been drawn for comparison purposes. Fig. 5 shows the effect of the change in the value of ω_0 on the contrast in the images. It is observed that

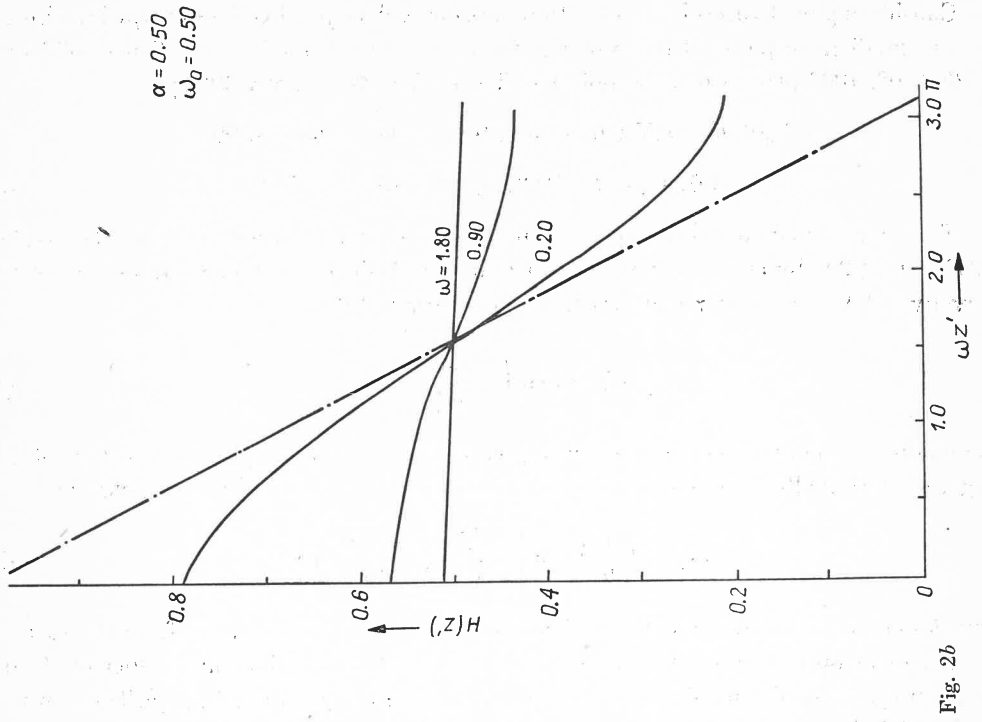
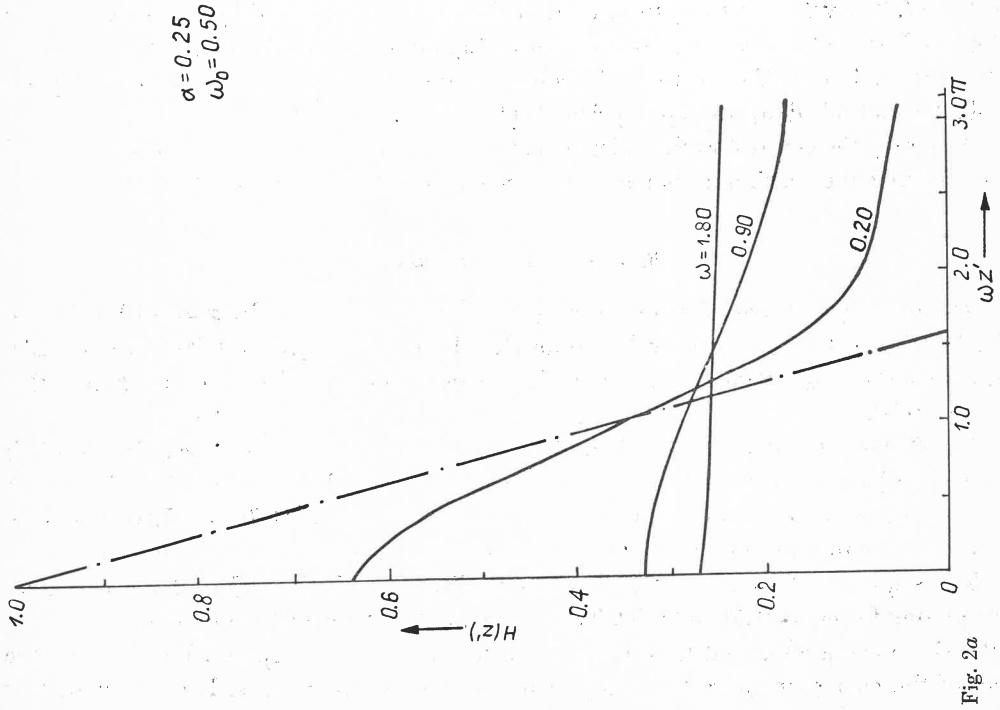


Fig. 2. Irradiances distribution in the images of the triangular wave objects. $\omega_0 = 0.50$. a) $\alpha = 0.25$ and b) $\alpha = 0.50$. ω in each case is 0.20, 0.90 and 1.80. Broken lines with dots (---·---·---) represent the edges of the geometrical images

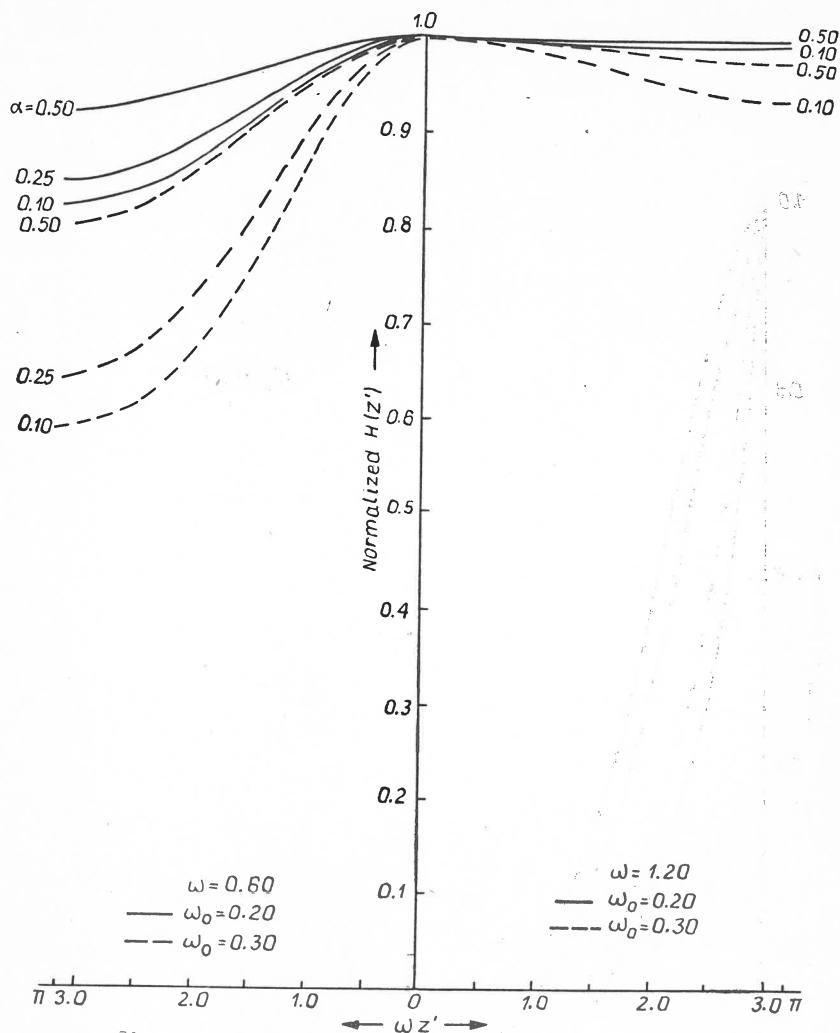


Fig. 3. Comparison of normalized irradiance distribution in the images for $\omega_0 = 0.20$ and 0.30 a) $\omega_0 = 0.60$ (—) b) $\omega_0 = 1.20$ (-----)
 $\alpha = 0.10, 0.25$ and 0.50 in each case for a)
 $\alpha = 0.10$ and 0.50 in each case for b)

a decrease in ω_0 results in a decrease of image contrast at all values of ω i.e. the image is degraded. Also, this decrease in the value of ω_0 results in the decrease of the value of the cut-off frequency.

The authors wish to thank Professor P. K. Katti and Professor M. S. Sodha for encouragement. Dr J. B. Goodell of Westinghouse Defence and Space Center, Maryland, sent us a copy of his manuscript in advance of publication and this is gratefully acknowledged. The suggestions of an anonymous referee contributed substantially toward improvements in the manuscript.

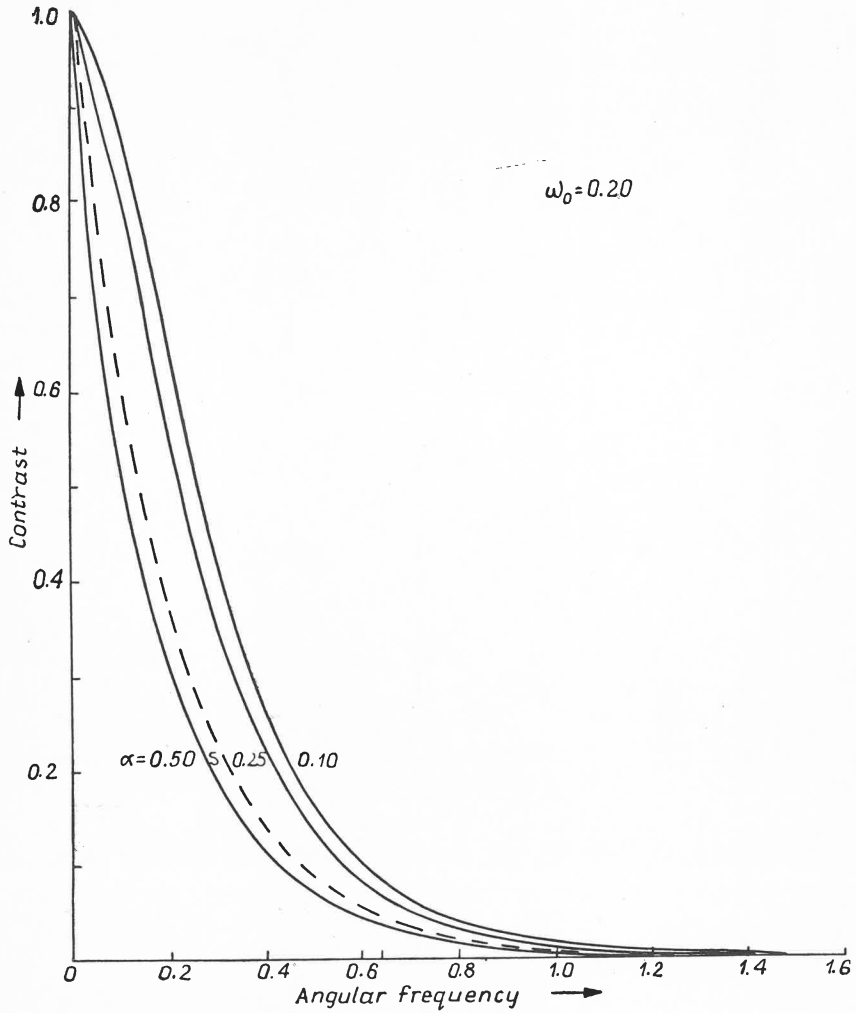


Fig. 4. Contrast in the images of the triangular wave object for a) $\omega_0 = 0.20$ and b) $\omega_0 = 0.50$. $\alpha = 0.10, 0.25$ and 0.50 in each case. Curves marked S give the contrast in the images of the sine wave object for corresponding value of ω_0

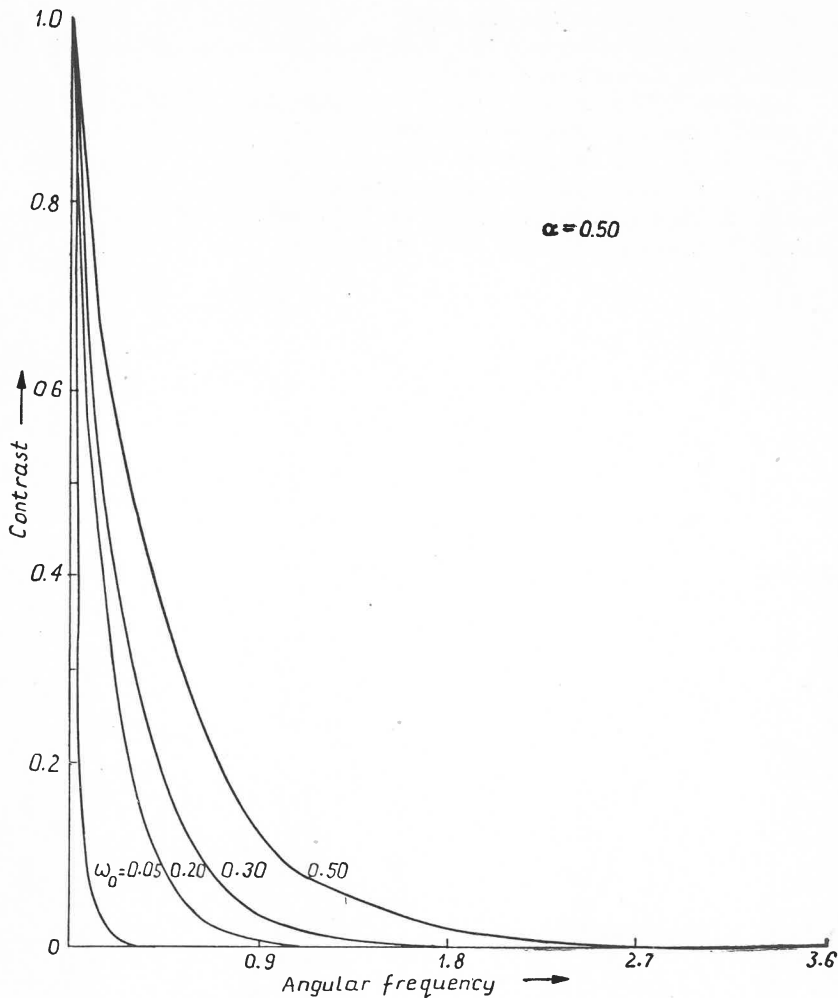


Fig. 5. Comparison of contrast in the images of the triangular wave object ($\alpha = 0.50$) for $\omega_0 = 0.05, 0.20, 0.30$ and 0.50

REFERENCES

- [1] W. E. Middleton, *Vision Through the Atmosphere* University of Toronto, Press Toronto, 1952.
- [2] J. Tyler, R. Preisendorfer, in: *The Sea*, Ed. M. N. Hill, Interscience Publ. John Wiley and Sons Inc., New York 1962, Vol. 1.
- [3] C. F. Beardsley, Jr., J. R. V. Zaneveld, *J. Opt. Soc. Amer.*, **59**, 373 (1969).
- [4] R. W. Preisendorfer, *Radiative Transfer on Discrete Spaces*, Pergamon Press (Ltd.), Oxford 1965.
- [5] N. G. Jerlov, *Optical Oceanography*, Elsevier Publishing Co., Amsterdam 1968.
- [6] S. Q. Duntley, *J. Opt. Soc. Amer.*, **59**, 472A (1969); Also see list of publications *J. Opt. Soc. Amer.*, **53** 213 (1963).

- [7] A. Ivanoff, *J. Opt. Soc. Amer.*, **59**, 472A (1970).
[8] F. W. Replogle, *Seminar Proceedings: Under Water Photo-Optics Society of Photo-Optical Instrumentation Engineers*, Santa Barbara 1966, p. A-V-1.
[9] J. R. V. Zaneveld, G. F. Beardsley, Jr., *J. Opt. Soc. Amer.*, **59**, 373 (1969).
[10] J. B. Goodell, *J. Opt. Soc. Amer.*, **59**, 477A (1969).
[11] W. H. Wells, *J. Opt. Soc., Amer.*, **59**, 686 (1969).
[12] K. Singh, K. N. Chopra, *Appl. Optics*, **8**, 1695 (1969).
[13] K. Singh, K. N. Chopra, *J. Opt. Soc. Amer.*, **59**, 1639 (1969).
[14] K. Singh, K. N. Chopra, *J. Opt. Soc. Amer.*, **60**, 641 (1970).